Adduct formation and energy redistribution
in UV and IR matrix-assisted laser desorption ionization

Akos Vertes[*a], Akos Bencsura[b], Mehrnoosh Sadeghi[a] and Xiongwu Wu[a]

[a]Department of Chemistry, George Washington University, Washington, DC 20052

[b]Chemical Research Center, Institute of Chemistry, H-1025 Budapest, Hungary

ABSTRACT

Molecular dynamics calculations were carried out to follow the first 100 ps of the plume formation in matrix-assisted laser desorption ionization (MALDI). Two specific issues were addressed: the desorption of guest species in the form of matrix adducts and some distinctive features of infrared (IR) MALDI. Co-desorption of guest and matrix ions in the form of an adduct was studied using positive substance P ions surrounded by sinapinic acid anions. Upon laser heating the surface layers of the matrix underwent phase transition and the adduct was transferred into the gas phase without decomposition. IR-MALDI was studied using succinic acid as a matrix in combination with triglycine guest molecules. The IR laser induced desorption process was modeled by coupling the succinic acid O-H bond to an external 900 K heat bath. The energy redistribution within the matrix molecules themselves and the transfer between the matrix and guest molecules resulted in an increase of the system temperature. The kinetic temperature of the matrix reached plateau at ~670 K within a few ps. The temperature of the guest molecule increased on a slower time scale and during the calculation the values remained several hundred K below the O-H vibrational temperature. The liftoff velocity of the guest species (~300 m/s) was similar to the values obtained in our previous calculations for different matrices and excitation methods.

Keywords: matrix-assisted laser desorption ionization, MALDI, mass spectrometry, ultraviolet, UV, infrared, IR, adduct formation, non-covalent complex formation

1. INTRODUCTION

Numerous biochemical processes utilize molecular recognition that, in turn, relies on the formation of non-covalent complexes between proteins and nucleic acids. Thus, the analysis of these species is of high importance. New and powerful bioanalytical methods are based on our ability to use mass spectrometry for the detection of these complexes, e.g., with matrix-assisted laser desorption ionization (MALDI).[1,2,3]

Molecular adducts can be held together by a variety of intermolecular forces. The strongest among these forces is the Coulomb interaction that attracts segments of the molecules carrying opposite partial charges. Complexes based on these, so called, ion pairs have been detected between peptides containing basic amino acid residues (Arg, His, Lys) and oligonucleotides containing the thymine (T) base. Similar ionic complexes can be formed between ionized peptides and oppositely charged matrix ions or their fragments. These complexes are called matrix adducts and are frequently observed in MALDI spectra. Although there have been considerable efforts for the molecular dynamics description of MALDI[4-9], the description of these supramolecular structures has not been attempted.

In order to gain insight into the behavior of these complexes, we studied the behavior of a matrix adduct during the MALDI process driven by a nitrogen laser pulse. The main questions we were trying to answer were related to the stability of the complex during the desorption process and to the conformation changes as the complex transferred from the solid phase to

---

the gas/vacuum environment. In this communication we describe the conformation changes of the adduct during laser heating and the consequences of the phase transition on the matrix and guest particles.

Although ultraviolet (UV) laser based MALDI is very efficient in the intact desorption and ionization of proteins, the MALDI of nucleic acids usually leads to partial fragmentation. To alleviate this problem, efforts are underway to develop potentially more gentle ionization methods based on MALDI utilizing infrared (IR) lasers.[10,11] While UV MALDI couples the laser energy to the sample via electronic excitation of the matrix, IR MALDI works through the direct heating of a vibrational mode of the matrix molecule. For example, the most used Er:YAG laser that works at 2.94 μm wavelength targets the stretching mode of the O-H bonds in the matrix molecules.

Molecular dynamics modeling of the IR MALDI process has not been attempted. Both our molecular modeling studies[4-6] and the breathing sphere model of Garrison et al.[8,9] are based on the uniform heating of the entire matrix molecule. This is an assumption that seems to be valid for UV MALDI where the electronic excitation of the matrix is quickly followed by internal conversion leading to indiscriminate heating of all its vibrational modes. Modeling of the IR MALDI process requires that one is able to selectively excite a particular internal degree of freedom and follow the fate of the deposited energy.

In the present communication we describe our preliminary results on the redistribution of internal energy during the IR MALDI process. Our particular concern is the efficiency of energy transfer between matrix and guest molecules during this process, as this energy transfer is responsible for the heating and ultimately for the fragmentation of the guest species.

2. MODELING METHODS

Similar to our previous studies on the leucine enkephalin—nicotinic acid system,[4-6] the c24b2 version of the molecular dynamics (MD) code CHARMM (CHARMM Development Project, Harvard University, Cambridge, MA) was used in the reported simulations.[12] Here we only elaborate on the differences between the methods in Refs. 4–6 and the present study. The empirical potential energy function adopted in CHARMM to model macromolecular systems, consists of the bond stretching, bending, improper dihedral, dihedral, van der Waals, and electrostatic terms. The "all atom" representation, in which every atom in the system was explicitly included in the calculations, was used throughout the simulations. In order to reduce the complexity of the MD simulations in the systems, reaction and fragmentation of the molecules were disregarded. The guest molecules, substance P, and triglycine, and the host molecules, sinapinic acid (SA), and succinic acid (SUCA) were represented using detailed descriptions of their molecular structures.
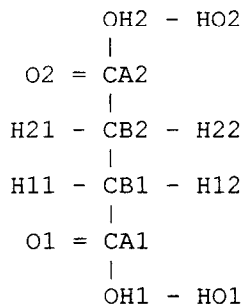
Partial charge distributions of the atoms in the structure of SA below were calculated using the GAMESS *ab initio* program for the fully optimized structure at the 6-31G* level:[13]
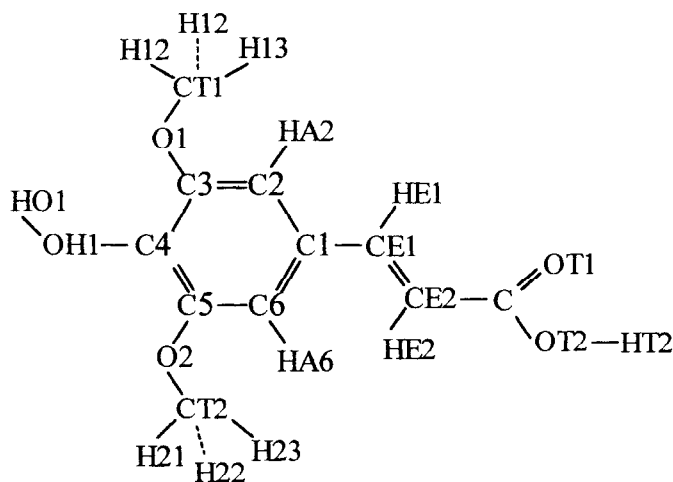
Table I. Atom types and partial charges in SA matrix molecules

Atom Number	Atom	Atom Type	Partial Charge
1	C1	CA	-0.15
2	HA2	HP	0.19
3	C2	CA	-0.26
4	H11	HA	0.10
5	H12	HA	0.04
6	H13	HA	0.04
7	CT1	CT3	0.05
8	O1	OS	-0.38
9	C3	CA	0.42
10	HO1	H	0.50
11	OH1	OH1	-0.63
12	C4	CA	-0.04
13	H21	HA	0.05
14	H22	HA	0.11
15	H23	HA	0.05
16	CT2	CT3	0.05
17	O2	OS	-0.47
18	C5	CA	0.51
19	HA6	HP	0.26
20	C6	CA	-0.43
21	HE1	HA1	0.15
22	CE1	CE1	-0.04
23	HE2	HA1	0.09
24	CE2	CE1	-0.13
25	C	CD	0.64
26	OT1	OB	-0.66
27	OT2	OH1	-0.58
28	HT2	H	0.52

The partial charge values provided in Table I were added to the CHARMM parameter file. Interaction parameters for SA were also estimated from similar compounds and groups in the CHARMM parameter files.

The crystal structure of SA was built based on X-ray diffraction data determined by Beavis and Bridson.[14] The SA crystal is described as monoclinic with P2$_1$/n symmetry having lattice parameters: a = 4.760(1) Å, b = 15.686(4) Å, c = 14.185(3) Å, and β = 90.30(2)°, a calculated density of 1.406 g/cm^3, and Z = 4. The CRYSTAL facility in CHARMM was used to build the initial crystal structure using the X-ray diffraction coordinates with the (103) plane positioned horizontally. The x-y dimensions of the crystal were 60.225 × 47.058 Å^2, containing 11 sheets of SA with 36 molecules in each sheet. To model a semi-infinite solid, two-dimensional periodic boundary conditions were applied to this cell. The two bottom layers were anchored to mimic the bulk of the crystal. In order to include the interaction of the fixed layers with the layer of molecules involved in the simulations, the number of the rigid layers was set so that their total thickness was less than the cutoff distance of the non-bonded interactions (13 Å). The 2-D periodic boundary conditions along the x-y plane and the rigid layers at the bottom allowed evaporation only at the top surface, perpendicular to the z axis.

IR-MALDI was studied using SUCA as a matrix in combination with triglycine, Gly$_3$ guest molecule. The structure and the atom assignments for the SUCA molecule are shown in the scheme below. Table II lists the partial charges on the individual atoms calculated by GAMESS at the 6-31G* level. The studied systems consisted of ~1200 matrix and 3-5 guest molecules with dimensions of approximately 60×80×33 Å^3. The IR laser-induced desorption process was modeled by coupling the O-H bonds of SUCA to an external heat bath. Heat bath temperatures ranging from 900K to 1100K represented different deposited laser energies.

Table II. Atom types and partial charges in SUCA matrix molecules

Atom Number	Atom	Atom Type	Partial Charge
1	HO2	H	0.48
2	OH2	OH1	-0.68
3	O2	OB	-0.60
4	CA2	CD	0.74
5	CB2	CT2	-0.06
6	H21	HA	0.06
7	H22	HA	0.06
8	CB1	CT2	-0.06
9	H11	HA	0.06
10	H12	HA	0.06
11	CA1	CD	0.74
12	O1	OB	-0.60
13	OH1	OH1	-0.68
14	HO1	H	0.48

```
            OH2  -  HO2
             |
     O2  =  CA2
             |
H21  -  CB2  -  H22
             |
H11  -  CB1  -  H12
             |
     O1  =  CA1
             |
            OH1  -  HO1
```

Due to the acidic environment of MALDI matrices, the basic amino acid residues (ArgH$^+$: pK$_a$ = 8.0, LysH$^+$: pK$_a$ = 10.0, HisH$^+$: pK$_a$ = 6.5) and the amino terminus (NH3$^+$: pK$_a$ = 8.0) of peptides and proteins are expected to be protonated.[2] Thus, for the UV study we chose the +3 charged ion of the naturally occurring undecapeptide, substance P, as the guest species:

NH$_3^+$ – Arg$^+$ – Pro – Lys$^+$ – Pro – Gln – Gln – Phe – Phe – Gly – Leu – Met – NH$_2$

Potential energy parameters for the amino acid residues were taken from the CHARMM parameter file. Since the substance P molecule carried three positive charges to maintain charge neutrality it was surrounded by three SA anions. In the SA anions, the HT2 atom on the carboxylic group was removed, thus, they were carrying negative charges. The matrix ions were then placed near to the charged groups of substance P, NH_3^+, Arg^+, and Lys^+. More precisely, the COO^- of the SA ions was placed in the vicinity of the hydrogen atoms of the amino terminus NH_3^+, and the hydrogen atoms of the end NH_2 and NH_3 in the side chains of Arg^+ and Lys^+, respectively. The system of substance P and SA ions, [Sub P^{3+} + 3SA$^-$], was energy minimized for 100 steps using the adopted basis Newton-Raphson method.

Two different host-guest systems were investigated, one with the complex on the surface of the SA crystal and another with an embedded complex. According to Ref. 14 in an SA crystal the extended hydrogen bonded sheets of SA molecules in the (103) plane are responsible for the protein inclusion. The protein molecules are assumed to attach onto the hydrogen-bonded sheets of the SA crystal, i.e., their hydrophobic portions become associated with the (103) hydrophobic face of SA.[14] In the first simulation the extended substance P and the three SA ions ([Sub P^{3+} + SA$^-$]) were positioned on top of the (103) surface of the crystal. The system was then equilibrated for 100 ps.

Layers seven to nine of matrix molecules from the equilibrated system were moved to the top of the [Sub P^{3+} + 3SA$^-$] species, creating the embedded system. The total number of SA layers, therefore, remained the same, eleven layers. The SA molecules within a radius of 2.4 Å were then deleted from the host crystal. This placed the guest molecule in the third layer of the embedded system. The [Sub P^{3+} + 3SA$^-$] complex extended into two layers. Afterwards, this system was equilibrated for 100 ps at 300 K. The laser excitation simulations were then carried out on the equilibrated host-guest systems.

Laser excitation of the systems was simulated by heating of the matrix molecules using the method introduced by Nose and Hoover.[15,16] Constant heat baths were coupled to the system and the heat flow rate from the heat baths to the systems was controlled by the appropriate assignment of two parameters, i.e., the thermal inertial momentum and the velocity of the scale parameter. Since the energy of the laser is mainly absorbed by the matrix molecules, a two-bath constant temperature method was implemented. Setting the properties of the two different heat baths allowed us to individually control the energy transfer to the guest and matrix molecules in a way that direct heating of the matrix molecules was achieved while guest species were only heated through their interaction with the matrix molecules. Gradual heating of the matrix, which is one of the factors that sets this study apart from previous simulations, is carried out at a rate that mimics the deposition of energy during the laser pulse.

In the UV study the temperature of the heat bath assigned to the matrix molecules during desorption was 2000 K, whereas the guest molecules were coupled to a 300 K bath. The thermal inertial momentum that controlled the rate of temperature fluctuations of the two heat baths was set to a value suggested by the CHARMM manual (10^{50}) to maintain a one-way continuous heat flow during the desorption process. The energy flow rate between the baths and the subsystems can be controlled by the velocity of the scale parameter, $\dot{s}$. In order to prevent the energy flow from the guest heat bath to the guest molecules, we set $\dot{s}_g = 0$ for the guest heat bath. However, to allow gradual energy flow from the matrix heat bath to the matrix molecules $\dot{s}_m = -0.001$ was selected. These parameter settings resulted in a system where energy transfer to the guest molecules only occurs through their interaction with matrix molecules. The typical time step for the simulations was 2 fs and the coordinates and velocities were saved at 0.2 ps intervals for later analysis.

The simulations were performed and analyzed on Indigo 2/R4400 and Indy/R4600 workstations operating under IRIX5.3 and IRIX6.2, respectively (Silicon Graphics, Mountain View, CA) and on a Sun Ultra Enterprise 4000 system (Sun Microsystems, Mountain View, CA) operating under SunOS 5.5.1. System structures and trajectories were visualized and monitored by SCARECROW (Centre for Scientific Computing, Espoo, Finland),[17] RasMol (Glaxo Wellcome R&D, Hertfordshire, U.K),[18] and MOLMOL (Institute of Molecular Biology and Biophysics, ETH, Zürich, Switzerland)[19] packages.

3. RESULTS AND DISCUSSION

To investigate a moderate size peptide guest species embedded in a widely utilized matrix, we studied the substance P–SA system. As mentioned, the three charges on substance P were located at the amino terminus and on the Arg and Lys residues. To achieve charge balance in the system, three SA anions were positioned around the guest particle. The substance P ion, complexed with the three SA anions, was put on the crystal surface and equilibrated for 100 ps at 300 K. The final conformation is shown in Figure 1. The three acid anions found their positions close to the charged sites in substance P. Each acid ion interacted with two charged sites of the substance P, essentially forming bridges. The charged sites were located near the N-terminus and, as a consequence, this part of the peptide was extended. At residues Gln5 and Gln6 there was a turn that arched the following section of the peptide away from the crystal surface. At residues Phe8 and Gly9 there was another turn which brought the C-terminal residue Met11 back to the surface.

After embedding the equilibrated guest complex, the substance P backbone changed its conformation and the turn near the C-terminus moved closer to the crystal surface. The SA anions occupied similar interaction positions with respect to the guest molecule and the entire complex extended over two crystal layers. The matrix molecules surrounding the guest complex were forced away from their original position and orientation, but the rest of the crystal structure did not change much.
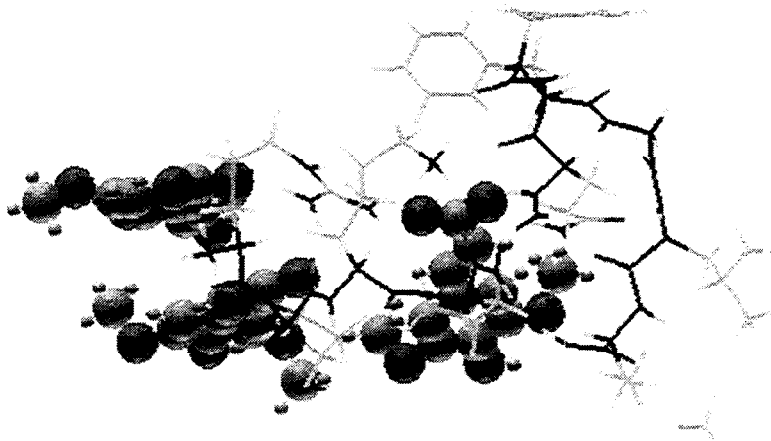
Figure 1. Ionized substance P molecule complexed with three SA counter ions at 300 K absorbed on the exposed (103) face of the SA crystal.

The laser excitation process was simulated with the Nose-Hoover method[15,16] by allowing energy transfer from heat bath to the matrix molecules. Starting from 300 K, we were able to observe the phase transition within the 100 ps of the simulation observing that the matrix crystal melted and evaporated turning into a gas. We observed that the guest species in the gas phase had a conformation very different from the one we found when it was adsorbed on or embedded into the matrix crystal.

Obtained from the simulation that started from the guest complex adsorbed on the surface, Figure 2 shows the gas phase conformation of substance P surrounded with the three acid anions. The turn in the peptide backbone at residues 8 and 9 disappeared. The new structure was basically a random coil with a loose turn at the middle and with the two ends moved closer to each other. Very significantly, all three acid anions stayed in the vicinity of the charged peptide sites.
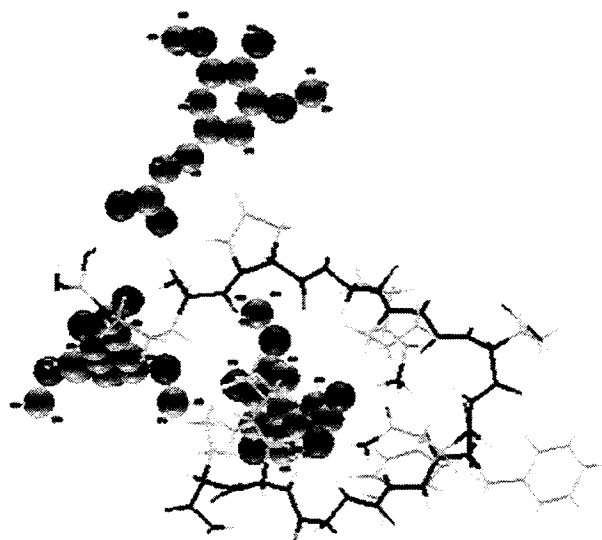
Figure 2. Substance P species stays complexed with the three SA anions during the desorption from the SA crystal surface.

To approximate a situation closer to MALDI, Figure 3 shows the gas phase conformation obtained from the system with the guest complex initially buried. The conformation of the desorbed species depended on the initial conditions of the simulation. This is an indication that in gas phase this relatively short peptide had more freedom to change conformation than on the crystal surface.
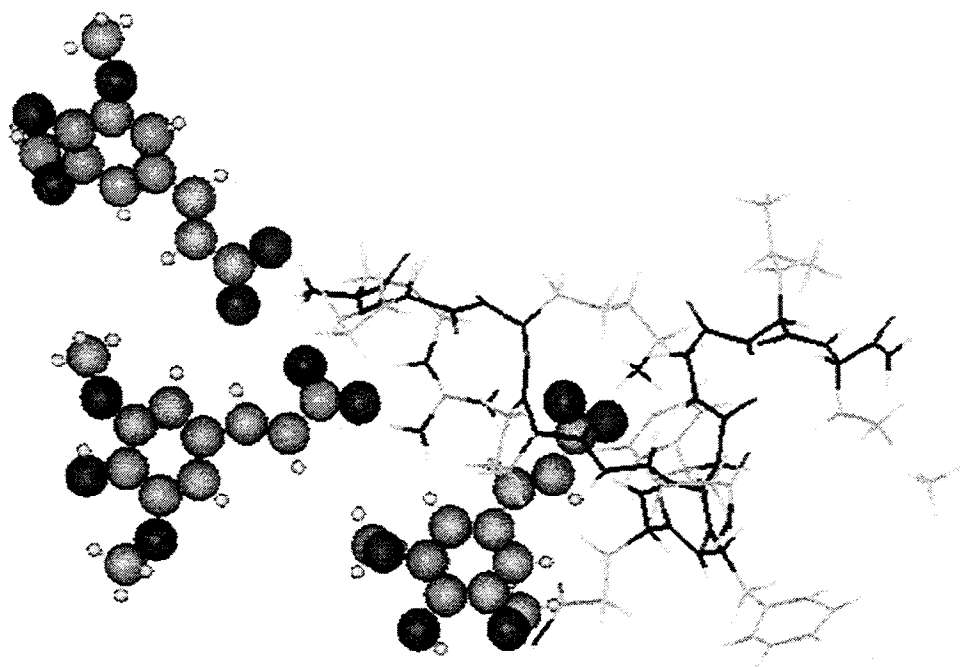

Figure 3. Gas phase conformation of substance P species with the three SA ions desorbed from the inside of the SA host crystal without decomposition.

Throughout and after the desorption, the three SA anions maintained their position relative to the substance P species, i.e., the [Sub P^{3+} + 3SA$^-$] complex was retained. Despite the energetic environment created by the laser irradiation, the

electrostatic interactions between the positive sites of substance P and the negative sites on the SA anions kept the complex from decomposition and the adduct transferred into the gas phase. This is in agreement with the observation that matrix–guest adduct peaks frequently appear in MALDI mass spectra. In fact, after protonated and alkalinated molecular ion peaks the matrix–guest adducts are among the most commonly observed peaks in MALDI mass spectra.

IR-MALDI was studied using SA as a matrix in combination with triglycine, Gly_3. The IR laser-induced desorption process was modeled by coupling the SA O-H bond to an external heat bath. Heat bath temperatures ranging from 900K to 1100K represented different deposited laser energies. The energy redistribution within the matrix molecules and the transfer between the matrix and guest molecules resulted in an increase of the system kinetic temperature. Figure 4 shows the effect of exciting the O-H bond to 900 K. The kinetic temperature of the matrix reached saturation within a few ps. The kinetic temperature of the guest molecule increased on a slower time scale and during the calculation the values remained several hundred K below the O-H vibrational temperature. The liftoff velocity of the guest species (~300 m/s) was similar to our previous calculations for different matrices and excitation methods.
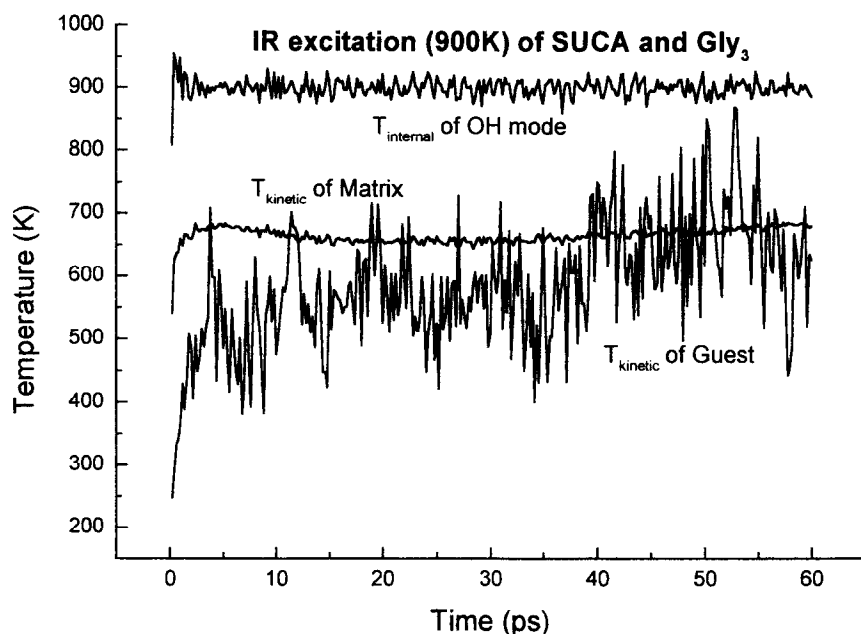

Figure 4: Internal and kinetic temperature histories of Gly_3 guest in SA matrix after IR excitation of the O-H bond to 900K.

In order to study the propagation of energy within a matrix molecule we studied the bond length distributions at different time stages. Figure 5 shows the distributions of the O-H bond and the neighboring bonds equilibrated at 300 K. As expected, the distributions are fairly narrow and resemble each other.
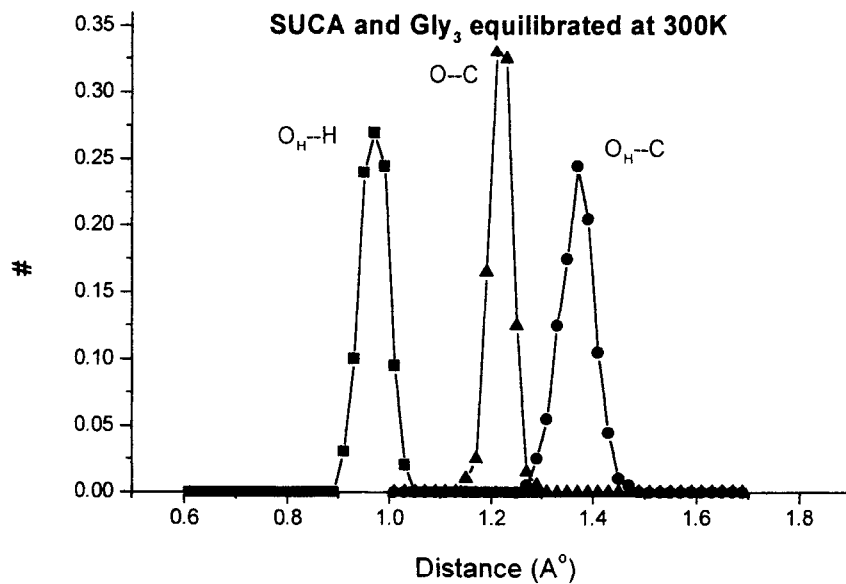
Figure 5: Bond length distributions equilibrated at 300 K before IR excitation of the O-H bond in SA.

In Figure 6 the length distributions of the neighboring C=O and C-OH bonds are compared with that of O-H after the IR laser excitation of the O-H bond. It is clear that at 35 ps the vigorous O-H vibrations have not subsided. It is also obvious that the O-H vibrations have very little influence on the length distribution of the neighboring bonds. This result is somewhat surprising and requires further study. The introduction of anharmonic potential terms is expected to facilitate the intra and intermolecular energy transfer.
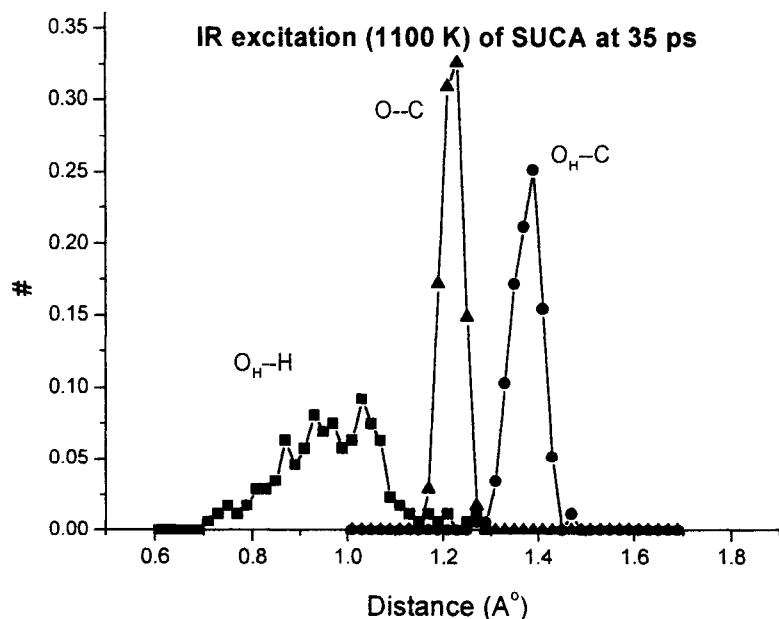
Figure 6: Bond length distributions at 35 ps after IR excitation of the O-H bond in SA with embedded Gly₃.

These results are in agreement with the data shown in Figure 4. Throughout the entire 60 ps of the simulation the O-H remained hot and the kinetic temperature of both the matrix and the guest were significantly lower.

ACKNOWLEDGMENTS

REFERENCES

1. P. Juhasz and K. Biemann, "Mass-spectrometric molecular-weight determination of highly acidic compounds of biological significance via their complexes with basic polypeptides," *Proc. Natl. Acad. Sci. U.S.A.*, **91**, pp. 4333-4337, 1994.

2. X. Tang, J.H. Callahan, P. Zhou, and A. Vertes, " Non-covalent protein—oligonucleotide interactions monitored by matrix-assisted laser desorption ionization mass spectrometry," *Anal. Chem.*, **67**, pp. 4542-4548, 1995.

3. A.S. Woods, J.C. Buchsbaum, T.A. Worrall, J.M. Berg, and R.J. Cotter, "Matrix-assisted laser desorption/ionization of noncovalently bound compounds," *Anal. Chem.*, **67**, pp. 4462-4465, 1995.

4. A. Bencsura and A. Vertes, "Dynamics of hydrogen bonding and energy transfer in matrix-assisted laser desorption," *Chem. Phys. Letters*, **247**, pp. 142-148, 1995.

5. A. Bencsura, V. Navale, M. Sadeghi, and A. Vertes, "Matrix-guest energy transfer in matrix-assisted laser desorption," *Rapid Comm. Mass. Spectrom.*, **11**, pp. 679-682, 1997.

6. X. Wu, M. Sadeghi and A. Vertes, "Molecular dynamics of matrix-assisted laser desorption of leucine enkephalin guest molecules from nicotinic acid host crystal," *J. Phys. Chem. B*, **102**, pp. 4770-4778, 1998.

7. L. Dutkiewicz, R.E. Johnson, A. Vertes and R. Pedrys, "Molecular dynamics study of vibrational excitation dynamics and desorption in solid O_2," *J. Phys. Chem. A*, **103**, 2925-2933, 1999.

8. L.V. Zhigilei, P.B.S. Kodali, and B.J. Garrison, "Molecular dynamics model for laser ablation and desorption of organic solids," *J. Phys. Chem. B*, **101**, pp. 2028-2037, 1997.

9. L.V. Zhigilei, P.B.S. Kodali, and B.J. Garrison, "A microscopic view of laser ablation," *J. Phys. Chem. B*, **102**, pp. 2845-2853, 1998.

10. S. Berkenkamp, F. Kirpekar, F. Hillenkamp, "Infrared MALDI mass spectrometry of large nucleic acids," Science, **281**, pp. 260-262, 1998.

11. M. Sadeghi, Z. Olumee, X. Tang, A. Vertes, Z.X. Jiang, A.J. Henderson, H.S. Lee, and C.R. Prasad "Compact Tunable Cr:LiSAF Laser for Infrared Matrix-Assisted Laser Desorption Ionization," *Rapid Comm. Mass. Spectrom.*, **11**, pp. 393-397, 1997.

12. B.R. Brooks, R.E. Bruccoleri, B.D. Olafson, S. Swaminathan, and M. Karplus, "CHARMM - A program for macromolecular energy, minimization, and dynamics calculations," *J. Comp. Chem.*, **4**, pp. 187-217, 1983.

13. M.W. Schmidt, K.K. Baldridge, J.A. Boatz, S.T. Elbert, M.S. Gordon, J.H. Jensen, S. Koseki, N. Matsunaga, K.A. Nguyen, S.J. Su, T.L. Windus, M. Dupuis, and J.A. Montgomery, "General atomic and molecular electronic-structure system," *J. Comp. Chem.*, **14**, pp. 1347-1363, 1993.

14. R.C. Beavis and J.N. Bridson, "Epitaxial protein inclusion in sinapic acid crystals," *J. Phys. D*, **26**, pp. 442-447, 1993.

15. S. Nose, "A unified formulation of the constant temperature molecular-dynamics methods," *J. Chem. Phys.*, **81**, pp. 511-519, 1984.

16. W.G. Hoover, "Canonical dynamics - equilibrium phase-space distributions," *Phys. Rev. A*, **31**, pp. 1695-1697, 1985.

17. L. Laaksonen, "A graphics program for the analysis and display of molecular-dynamics trajectories," *J. Mol. Graph.*, **10**, pp. 33-65, 1992.

18. R. Sayle, *RasMol V2.6, Molecular Visualization Program*, GlaxoWellcome Research and Development, Stevenage, Hertfordshire, U.K., 1992.

19. R. Koradi, M. Billeter, and K. Wüthrich, "MOLMOL: A program for display and analysis of macromolecular structures," *J. Mol. Graphics*, **14**, pp. 51-58, 1996.